AFRC 2024 Industrial Combustion Symposium
Calgary, Alberta Canada
September 30 – October 03

Assessment of Natural Gas Substitution with Hydrogen on Heat Transfer and NO_x Emissions

Chaimae Bariki, Bernard Labégorre, Benjamin Le Creurer
Air Liquide, Innovation Campus Paris, 1 chemin de la Porte des Loges, Les Loges-en-Josas, France

Abstract

In the frame of the efforts made by the industry to reduce its CO_2 emissions, the replacement of natural gas (NG) with decarbonized hydrogen (H_2) as a fuel in combustion applications (glass melting and steel reheating, among others) is one of the promising options. However, such a change brings several technical challenges which need to be thoroughly addressed. Amongst these challenges are assessing the capability of existing burners to operate with hydrogen in order to comply with the industrial processes, and define strategies for optimization and/or development of new concepts. Two approaches exist based on experiments and numerical simulations, which complement one another. The latter has made significant progress in the last decades, and is more and more employed. Nevertheless, the obtained results are strongly dependent on the models used and a validation stage is thus mandatory against experimental data.

The main objective of the present paper is to discuss the numerical results obtained with NG substitution by H_2 on the heat transfer to the load and NO_x emissions generated by oxy-flames. A validation step was necessary using NG experimental data measured in the Air Liquide pilot furnace, which was designed to test oxy-burners up to 2 MW thermal inputs in a thermal environment representative of many high/medium temperature industrial furnaces. CFD simulations were performed using the ANSYS-Fluent software and a dedicated set of wsgg-coefficients for the radiation model was used.

Keywords: H_2 oxy-combustion; Separated jet burner; Radiation; NO_x emissions; Heat transfer

1. Introduction

Owing to ever more stringent regulations and the rising costs of primary sources, the energy-intensive manufacturing processes of various sectors (e.g. the glass or steel industry) are obliged to use alternative energy sources to produce as sustainable as possible. In such industry sectors, the oxy-fuel combustion of natural gas (NG) is a well established process. By using oxygen instead of air as an oxidizer, significantly higher efficiencies are obtained due to the increased peak flame temperatures and the lower overall flue gas mass flow. While higher oxy-fuel furnace efficiencies already reduce CO_2 emissions, further substituting natural gas by zero-carbon fuel, such as hydrogen (H_2), can significantly reduce CO_2 emissions close to zero, depending on the source of the hydrogen used. Therefore, the combustion properties of hydrogen need to be thoroughly investigated, especially in terms of radiation properties and NO_x pollutant formation mechanisms.

Heat radiation is the primary mode of heat transfer in high-temperature combustion environments, which can be generated by the flame itself and its hot flue gases, and the walls of the furnace. Several studies have been conducted to assess the respective contribution of these sources to the overall radiation. In particular, it was shown that the contribution from the flame highly depends on the presence of soot particles, but the impact is mainly local [1]. Since it is often difficult to evaluate

radiative heat transfer experimentally, radiation modeling is an important alternative. In CFD simulations for industrial configurations, the emissivity of a gas mixture is usually approximated using a Weighted Sum of Gray Gases (WSGG) model [2][3]. Most of the existing WSGG models have been validated for natural gas combustion with air or oxygen and are therefore not applicable to hydrogen oxy-combustion due to the high content of water vapor which leads to a different emission spectrum of the exhaust gas. The fundamental challenge in the WSGG model lies in determining the weights and absorption coefficients of the various gray gases. Air Liquide R&D developed expertise over the years [4] and proposed a dedicated set of coefficients to accommodate hydrogen oxy-combustion applications, which were used in the present work.

Nitrogen oxides (NO_x), produced as byproducts during the combustion process, represent a significant threat to the environment. NO_x emissions, comprising mainly nitric oxide (NO) and smaller amounts of nitrogen dioxide (NO_2), contribute to ozone depletion, cause the production of photochemical smog, and are dangerous to human health. The need to comply with stricter emission regulations is, therefore, mandatory. NO_x emissions can be drastically reduced when oxygen is used as an oxidizer. The elimination of air-borne nitrogen generates a flue gas that mainly consists of carbon dioxide and water, theoretically. In industrial furnaces, NO_x emissions can still be formed because of: (1) air-ingress in the combustion chamber, (2) the presence of molecular nitrogen traces in the oxygen stream, and (3) the oxidation of fuel-bound nitrogen (e.g. ammonia (NH_3), natural gas with negligible N_2 amounts). The chemical mechanisms controlling NO formation are well known [5][6], and their relevance depend on the operating conditions and the fuel used. Turbulence, on the other hand, directly affects NO formation rates because of the complicated mixing process and the varying residence time that could favor NO_x formation. The chemistry/turbulence interaction is complex and its effect on NO formation needs to be carefully investigated [7][8].

To address the above mentioned points, Air Liquide follows a two-step strategy:

1. Develop a better knowledge on H_2 combustion when switching from NG to H_2 oxy-combustion to upgrade and develop new burner technologies. For this, experiments are conducted at Air Liquide R&D test platforms using its various pilots (lab- to semi-industrial scale), together with advanced CFD simulations.
2. Conduct trials with industrial partners (e.g. a Japanese glassmaker during 2023 and SGD Pharma in France early 2024, among others) to assess the impact of fuel switching in real industrial environments [10].

The main objective of the present paper is to discuss the numerical results obtained with the ALGLASS FC burner, one of the most referenced Air Liquide burners, when switching from NG to H_2. A validation step was necessary using NG experimental data measured in the Air Liquide pilot furnace, which was designed to test oxy-burners up to 2 MW thermal inputs in a thermal environment representative of many high/medium temperature industrial furnaces. CFD simulations were performed using the ANSYS-Fluent software using a dedicated set of WSGG-coefficients for the radiation model.

2. Numerical framework

One of Air Liquide's pilot furnaces was designed to test burner thermal inputs ranging from 500 kW to 2 MW (cf. Figure 1). The specificities of this furnace are: (1) the maximum operating temperature of 1600°C allows testing oxy-burners in a thermal environment representative of many high/medium temperature industrial furnaces, (2) the heat load is simulated using 13 water-cooled panels installed at the bottom of the furnace. Detailed characterization of the heat extraction profiles can be obtained, (3) heat extraction and furnace outlet temperature can be varied by insulating the sides of the

water-cooled furnace floor, and by covering part of the water-cooled panels with a radiative screen consisting of silicon carbide (SiC) panels to simulate high-temperature thermal load, as in industrial applications, and (4) an electrically motorized damper is located in the chimney to control the pressure of the combustion chamber so that air ingress within the furnace can be limited.

Figure 1 - One of Air Liquide's pilot furnaces.

The ALGLASS FC burner is a staged burner comprising separate injections of fuel and oxygen, as sketched in Figure 2. At the lower stage, the fuel is distributed in the three inner pipes, each one surrounded by a small amount of oxygen. The fuel pipes are arranged in a fan-shaped configuration, so that the streams of fuel form a wide planar jet of gas in the furnace. At the upper stage, oxygen is injected at lower velocity through two lances tilted by a few degrees to direct the oxygen flow towards the fuel jets.

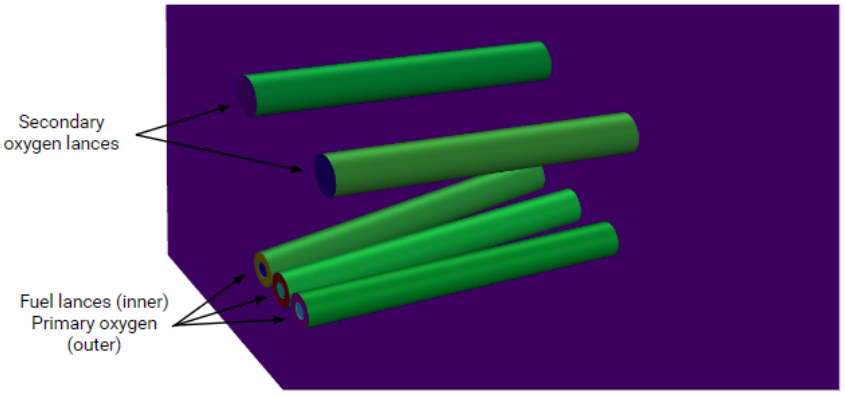

Figure 2 - ALGLASS FC 1000 burner.

2.1. Mesh generation

The meshing strategy used is described as follows: three domains (known also by body of influence 'boi') are created in order to control the mesh size generated and therefore limit the total number of mesh cells. The idea is to start with a highly refined mesh near the burner block at areas which are necessary to have more elements to better resolve the rapid changes in the flow, and ending up with coarser mesh cells at the chimney. Requirements on expansion ratios are made to ensure a resulting mesh with good quality. For that matter, a common CFD rule of thumb is to limit cell size expansion to 20% between neighboring cells. In this work, an expansion ratio of 4% and 10% are applied between the blocks. Boundary layer mesh is generated close to the wall, with a different requirement on the mesh y^+ depending on the turbulent model used. Polyhedral meshes are generated and the total cell

number is about 2 millions (cf. Figure 3). Note that this mesh was obtained after several trials and was found to be a good compromise between accuracy and computational time.

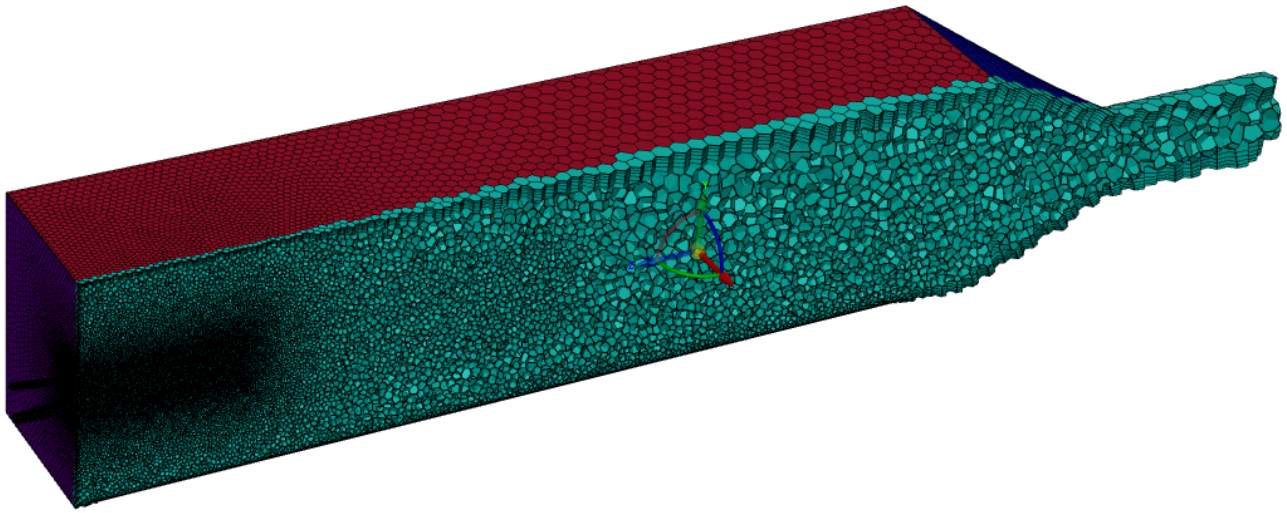

Figure 3 - Exemplary image of the generated mesh using the strategy described above.

A good mesh quality is essential for performing a good CFD analysis. Therefore, assessment of the mesh quality before performing large and complex CFD analysis is very important. Low skewness and high orthogonal quality are recommended. In our case, a skewness of 0.011 and an orthogonal quality of 0.96 are obtained with the generated mesh.

2.2. Physical models

Steady RANS simulations were carried out using the ANSYS Fluent 2023 R2 solver. It is noteworthy that the choice of models to be solved is a key point for a good understanding of phenomena occurring in the combustion chamber. In the present work, combustion is solved with the non-premixed model which is specific to turbulent diffusion flames with infinitely fast chemical kinetics. Since combustion in the furnace is governed by turbulence mixing, two turbulence models were tested: *i*) the realizable *k-ε* model with enhanced wall function and *ii*) the shear stress transport (SST) *k-ω* model known for their robustness and accuracy especially in the boundary layers. Radiative heat exchanges between the flame, flue gases and walls are solved by the discrete ordinate (DO) method together with one of the weighted-sum-of-gray-gases models (WSGG), which are: Fluent-WSGG, AL13-WSGG and AL22-WSGG. The last two models were specifically developed by Air Liquide R&D to accommodate oxy-combustion applications. NO formation via the thermal route is predominant in the oxy-fuel combustion resulting in high flame temperature. Therefore, only thermal NO_x is considered in the present study. Note that this model is based on the extended Zel'dovich mechanism in Fluent.

2.3. Boundary conditions

Uniform inlet velocities are imposed at the inlet of fuel and oxygen injection surfaces and the pressure outlet condition is imposed at the outlet. The NG composition was obtained from a chromatography analysis. For the H_2/O_2 case, a composition of oxygen produced from an on-site production unit is considered which contains about 3% of nitrogen. This allows investigating NO_x emissions generated during the combustion process. Refractory walls and windows around the furnace are associated with constant heat transfer coefficients, h_w. Note that the local heat flux lost through the wall,

$\phi = h_w\left(T_w - T_\infty\right)$, is proportional to the difference between the surface temperature inside the furnace, T_w, and the temperature of the ambient air outside the furnace, T_∞.

2.4. Convergence

The pressure-based solver is used to solve the steady equations for mass, momentum and energy balance (Navier-Stokes equations). To ensure that simulations have converged, i.e., equations are satisfactorily solved, several criteria are defined: (1) residuals below 10^{-6} for energy, mean mixture fraction and radiation equations, and 10^{-3} for all other equations, (2) mass imbalance $\ll$ 1% and energy imbalance < 1%, and (3) targeted quantities, which are the furnace exhaust temperature, crown temperature and heat transferred to the load, converge towards an asymptotic value. Oscillations obtained were below 1% for the heat flux and below 2 K for temperature.

2.5. Selected conditions

The investigated conditions are summarized in Table 1.

Table 1 - Investigated conditions.

	Simulated Cases		Available Experimental Data			
	Case	Power (kW)	T_{crown} (K)	T_{fumes} (K)	Heat Transfer (kW)	NO_x Emissions (ppm)
NG / O_2	NG-600	600	**x**	**x**	**x**	**x**
	NG-1000	1000	**x**	**x**	**x**	**x**
	NG-1500	1500	**x**	**x**	**x**	**x**
	NG-1750	1750	**x**	**x**	**x**	**x**
H_2 / O_2	H_2-1000	1000	–	–	–	–

3. Results & Discussion

3.1. Numerical model validation

This section covers results obtained with the ALGLASS FC burner for NG/O_2 cases at 1000 kW firing rate. Unless stated otherwise in this section, the *k-ε* realizable model is used for turbulence and the AL13-wsggm is used together with DO for radiation.

3.1.1. Temperature distribution and profiles

The flame temperature contours at the vertical and horizontal mid-planes of the furnace are shown in Figure 4. One can see that the flame is relatively long and bends towards the bottom of the furnace with a maximum temperature of ~2500°C and an average temperature in the furnace of 1300°C. The flame bending is explained by the secondary oxygen lances which are tilted downwards, directing the jet towards the bottom.

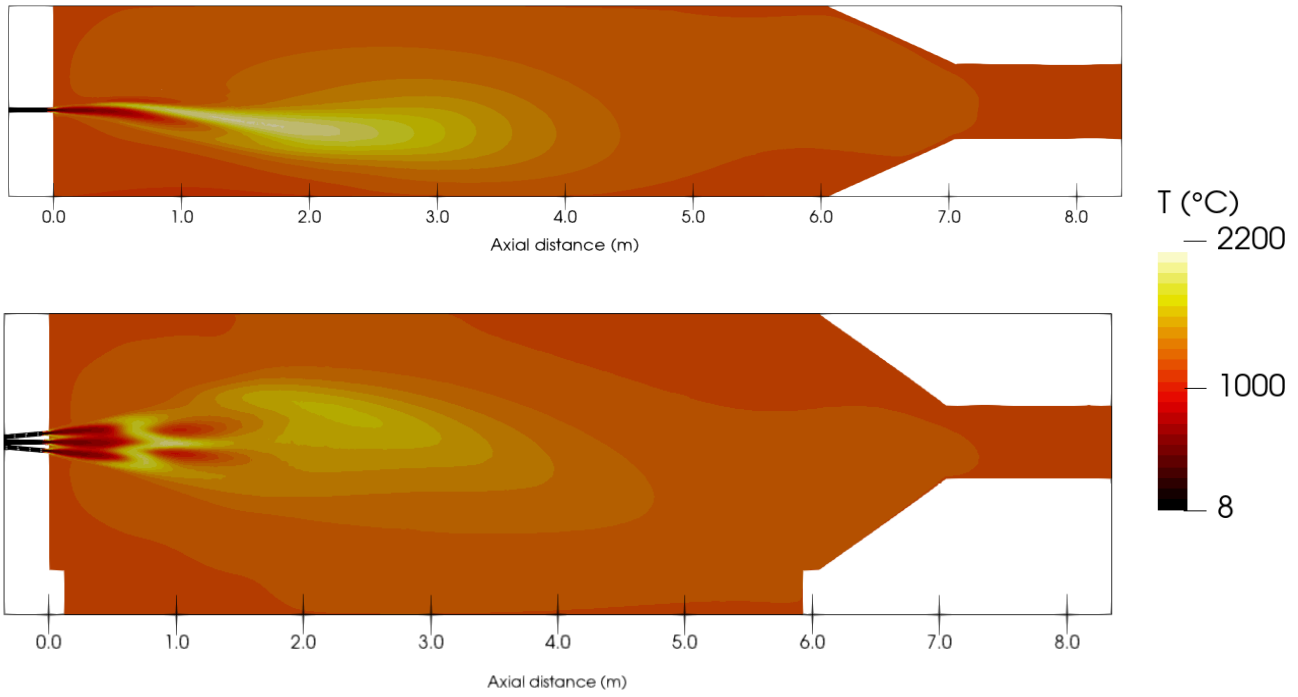

Figure 4 - 2D temperature contours at the vertical (top) and horizontal (bottom) mid-planes of the furnace. Burner thermal power: 1000 kW.

Temperature profiles at the furnace crown along the furnace and at two radial positions, namely at z = 1 m and 2.5 m, are analyzed in Figure 5. The numerical model gives satisfactory results when compared to experiments at firing rates of 600 kW and 1000 kW. However, it under-predicts the experimental data of about 100°C at higher thermal powers, where the maximum is located. It is worth pointing out that, given the furnace's good thermal insulation, the temperature variations observed lead to only slight variations in heat flux compared to the heat released in the flame or the flux transferred to the floor.The sudden decrease of temperature measured at 3 m for the four firing rates is most likely linked to a different position of the thermocouple in the furnace, and therefore the decrease has most likely no physical explanation related to flow or flame properties. This could be improved in the future.

For completeness, the averaged temperature at the furnace exit is also compared with experimental data and the results are shown in Figure 6. The predicted temperatures are in a very good agreement with experiments (less than 40°C). Regarding the furnace heat losses, these are negligible compared to the heat transferred to the load and the flue gas energy at the outlet. It is important to highlight that a fair/correct comparison between experiments and simulations requires the following:

- Mass and energy balances for measurements should be systematically evaluated. These were not available for the operating conditions investigated in the present study, which make it difficult to explain the differences obtained between experimental and numerical data at high thermal powers.
- Measurement uncertainties need to be correctly defined. These were also not documented in the past, but should be included in future experiments.

The position of the burner in the furnace needs to be specified because it can have a direct impact on the flow field.

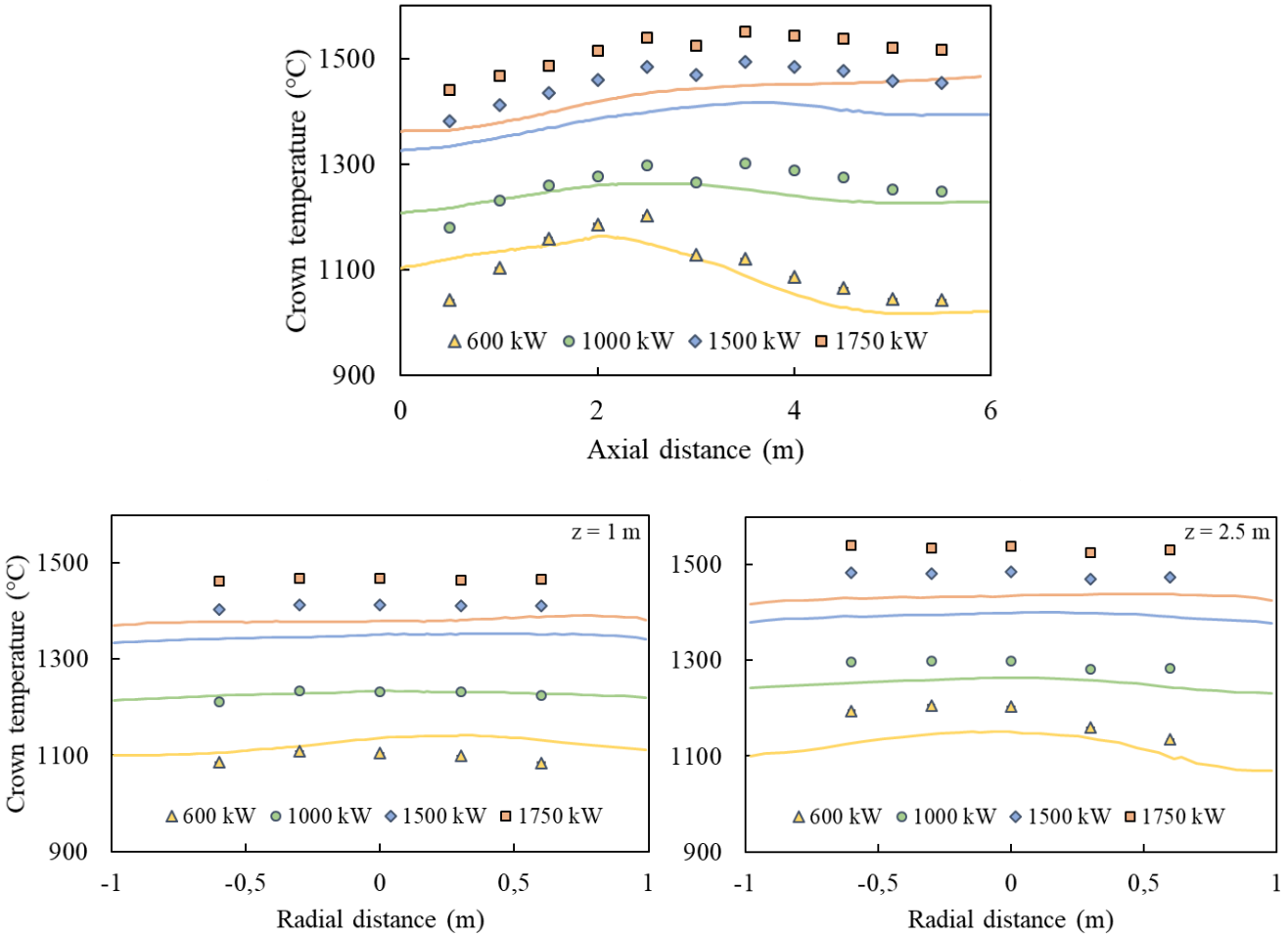

Figure 5 - Crown temperature profiles at different firing rates along: (top) the mid-planel axis of the furnace and (bottom) two radial positions: z = 1 m and z = 2.5 m. Symbols and lines represent experiments and simulations, respectively.

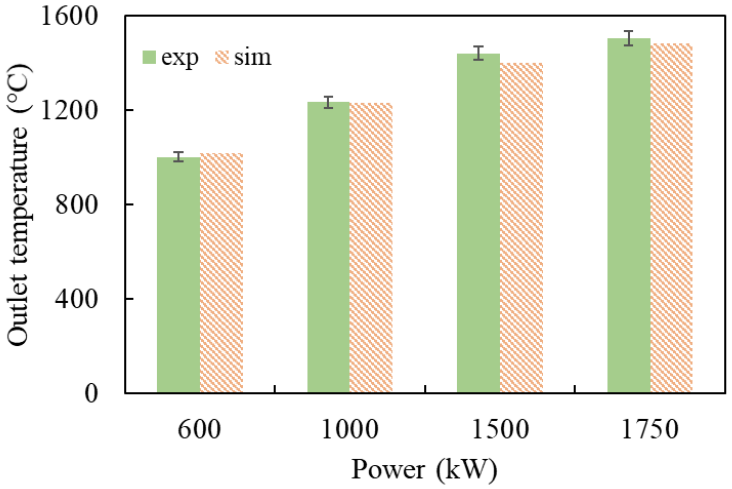

Figure 6 - Temperature at the furnace outlet at different firing rates.

3.1.2. Heat transfer to the load

Figure 7 presents a comparison of the total heat transfer to the load obtained with experimental and numerical data. For experimental data, an error bar has been added, representing the uncertainties

related to the water temperature variations. A good agreement is observed between experimental and simulation results. The heat transfer to the load increases as the burner thermal power increases. The relative errors calculated are between 3 and 10% at 1000 kW and 1750 kW, respectively.

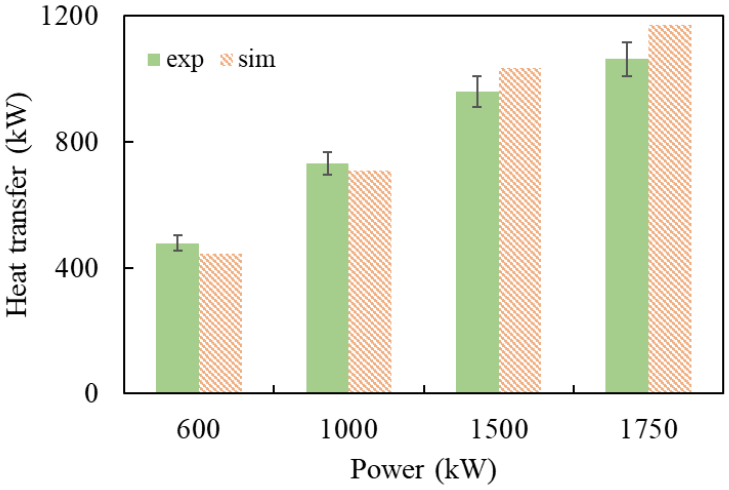

Figure 7 - Experimental and numerical heat transfer to the load as a function of the burner thermal input.

Let's have a closer look at heat transfer profiles extracted along the floor of the furnace to evaluate the numerical model at various firing rates. Two main outcomes can be drawn from Figure 8:

1. The numerical model captures the increase of the heat transfer to the load while the firing rate is increased.

2. Experimental and numerical data are in a good agreement at 600 kW and 1000 kW firing rates. Nevertheless, an overprediction up to 3% at 1500 kW and 8% at 1750 kW (as the maximal relative error) is observed with simulations. The peak position is also shifted and is located at the second-half of the furnace, at approximately 3.5 m downstream of the burner.

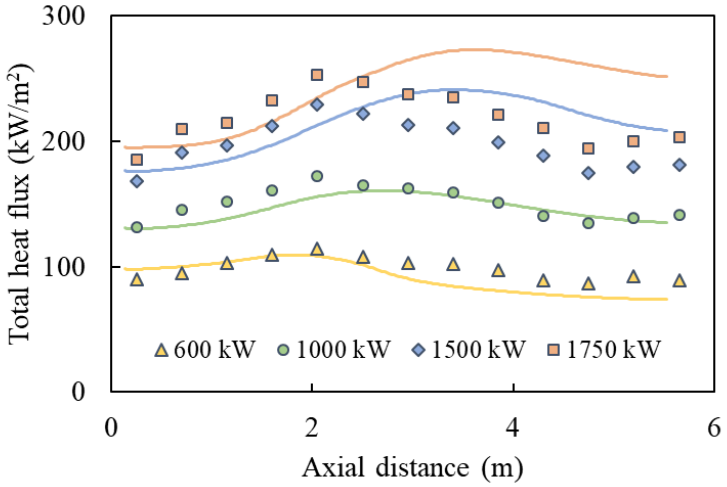

Figure 8 - Heat flux evolution along the furnace floor at different firing rates. Symbols and lines represent experiments and simulations, respectively.

In order to investigate the peak shift of the heat transfer identified while increasing the firing rate, *i.e.* at 1500 kW and 1750 kW, two different explanations are identified:

- The burner could be slightly off-center during experiments. Therefore, this could impact the flowfield, especially the location where recirculation zones are created. Since the burner position was not defined in the experimental report, this point has not been further investigated. However, a parametric study could be helpful to better understand the effect of this parameter on the flowfield.

- The near-wall law is not taken into account properly. To investigate this, additional simulations were conducted using the *k-ω* SST turbulence model. The obtained results (not presented here) showed that turbulence models used in this work do not fully capture the same flowfield. This suggests that a re-examination of the turbulence modeling with an appropriate near-wall law is required, especially for the *k-ε* realizable model, with a proper y^+.

3.1.3. NO_x emissions

NO_x formation is predicted in a post-processing mode with the flow field, temperature, and species concentrations fixed. This mode is justified on the grounds that the NO concentrations are very low and have negligible impact on flame and flow properties. Therefore, only the NO_x mass balance equation is computed. Here, only thermal NO model was activated since it is predominant in oxy-diffusion flames [9].

The NO rate contour at the vertical mid-plane of the furnace is shown in Figure 9. The temperature iso-contour at 1800°C (representative of the flame front reaction zone) is displayed with a white line. One can see that nitrogen oxides are produced in the flame at high temperatures above 1800°C. This finding holds true for cases at different firing rates.

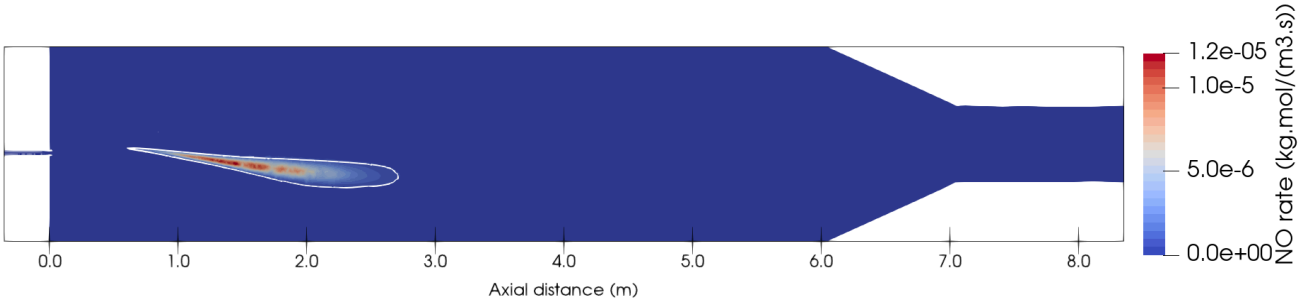

Figure 9 - NO rate[1] contour at the vertical mid-plane. The iso-temperature at 1800°C is overlaid. Thermal power: 1000 kW.

The predicted NO_x emissions normalized at 3% of oxygen content obtained at the furnace outlet are compared with those measured experimentally in the flue gases, and are shown in Figure 10. The main points that can be drawn are:

- Based on experimental data, NO_x emissions depend strongly on the furnace temperature and increase as the temperature increases. This trend is also well captured by the numerical model.

- The NO model underpredicts the emissions at low furnace temperature, while it overpredicts (up to 50%) the emissions at high furnace temperatures. Note that the 1000 kW operating condition was used to calibrate NO_x predictions against experimental data.

[1] NO rate in kg.mol/(m^3.s)

- Differences obtained between simulations and experiments can be explained by turbulence fluctuations which differ from one case to another depending on the operating conditions and therefore the magnitude of these fluctuations. Despite the substantial differences, the model can predict the trends correctly. Qualitative analyses are hence possible to improve the burners design.

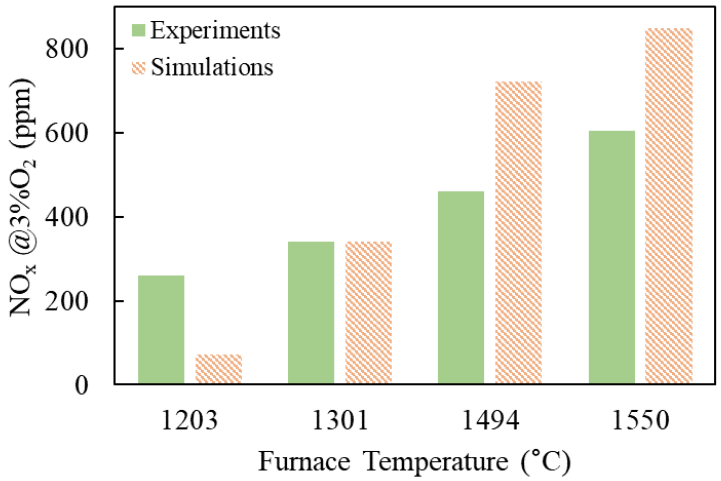

Figure 10 - Comparison between experimental and numerical NO_x emissions obtained at various firing rates.

It can be concluded so far that the numerical model captures the physics correctly despite the differences identified in terms of NO_x emissions, and is good enough to investigate the effect of switching from NG to H_2. Several possible leads are identified to further improve the model in general (e.g. re-examination of turbulence modeling, calibration of wall BCs with the pilot furnace, burner position sensitivity).

3.2. Effect of NG substitution with H_2

Substitution of hydrocarbon fuels with hydrogen produced from renewable resources can be used to decarbonize several sectors. However, the high reactivity and high diffusivity of hydrogen is expected to modify the flame dynamics consequently. In order to assess the effect of hydrogen addition to natural gas numerically, it is crucial to use the same physical models to isolate the impact of fuel change. A comparative analysis has been performed first to evaluate the differences between the WSGG models since radiation plays an important role. It was found that the AL models, which were developed specifically for oxy-combustion applications, give similar results. Therefore, the AL22-WSGG model is used hereafter since it is valid for any CH_4/H_2 blend ratio.

Two cases were investigated: the fuel can be pure natural gas or pure hydrogen. For both simulations performed, all physical models were kept the same and only the species' PDF table was different for each case. Note that no experimental data were available and therefore the assessment is done based only on CFD results.

3.2.1. Heat transfer to the load & Crown temperature

The heat transfer profiles along the floor of the furnace are first evaluated. Figure 11 represents the obtained results for the two reactive mixtures. The main takeaways are:

- Adding hydrogen to NG has clearly an impact on the heat transferred to the load. A 10% increase in the heat flux is identified at the position where the maximum is reached for H_2 case.

- The heat flux distribution over the floor looks different when comparing pure hydrogen and pure NG cases. It can be seen that the heat transfer to the load is more important in the first half of the furnace than the second half with the oxy-hydrogen flames, while it is more homogeneous with the oxy-NG flame.
- Although the heat transfer distribution along the floor is different when adding H_2 to NG, the total heat transfer obtained is quite similar. An increase of less than 2% is obtained when adding H_2 (cf. Table 2).

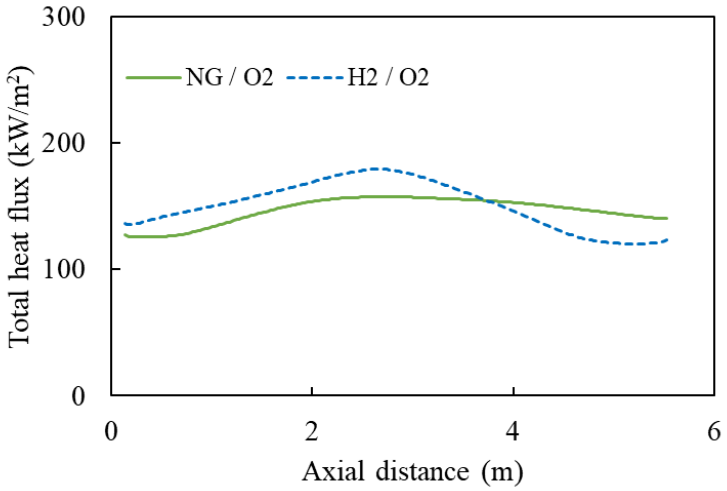

Figure 11 - Heat flux evolution along the floor of the furnace at various operating conditions: NG/O_2 and H_2/O_2, heat duty of 1000 kW.

Temperature profiles along the crown of the furnace are evaluated (cf. Figure 12). Differences up to maximum 45°C are obtained between pure NG and H_2 cases. The resulting flue gas temperature at the outlet slightly decreases for H_2 firing cases (cf. Table 2). This is consistent with the relatively high heat transfer to the load observed in the first half of the furnace.

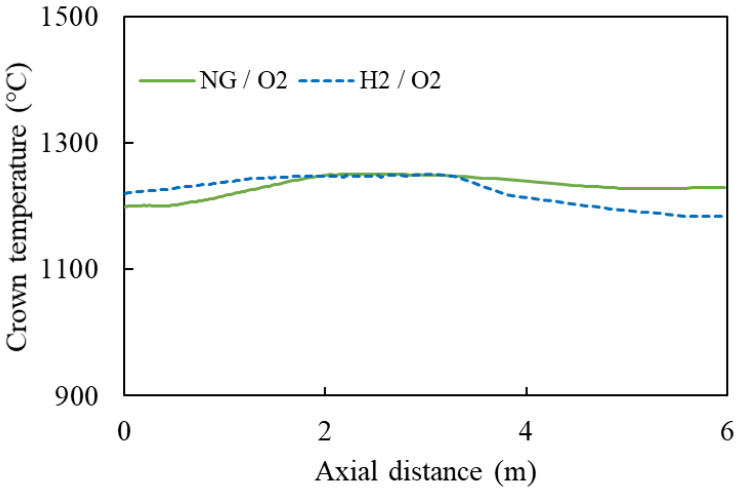

Figure 12 - Crown temperature profiles at various operating conditions: NG/O_2 and H_2/O_2, heat duty of 1000 kW.

Hydrogen is known to enhance flame stability and temperature. The maximum temperature reached in the furnace is evaluated (cf. Table 2). As expected, the temperature increases when switching from pure NG to pure H_2.

Table 2 - Key parameters obtained with CFD simulations.

Composition	NG / O_2	H_2 / O_2
Maximum temperature (°C)	2496	2577
Temperature at the exit (°C)	1230	1209
Heat transfer to the load (kW)	708	720

3.2.2. NO_x emissions

NO contours at the vertical furnace mid-plane together with the iso-temperature at 1800°C, which represents the flame reaction zone, are displayed in Figure 13 for the two reactive mixtures investigated. It can be seen that *i*) the pollutants are formed in the flame region and *ii*) an increase in hydrogen content leads to a shortening of the flame due to different mixing effects.

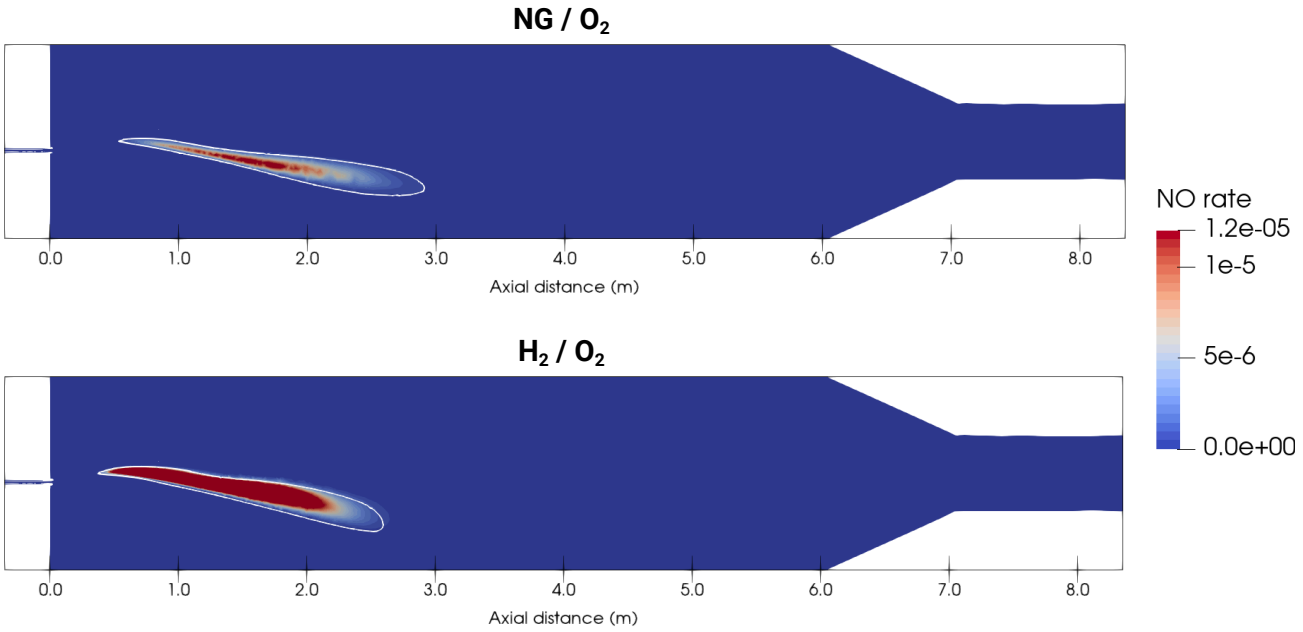

Figure 13 - NO rate contours at the vertical mid-plane for mixtures investigated: (top) NG/O_2 and (bottom) H_2/O_2. The iso-temperature at 1800°C is overlaid. Burner thermal power: 1000 kW.

NO_x emissions, on a dry basis, normalized at 3% of oxygen content are calculated at the furnace outlet. Before discussing the results, it is important to highlight that direct comparisons of pollutant concentrations in ppm, which is a common practice used within the combustion community, can lead to an apparent increase in emissions for H_2-blended fuels relative to strictly hydrocarbon fuels. While fuel-dependent pollutant formation mechanisms may also play an important role in relative emissions rates, the results emphasize that the increased concentration of water and oxygen in the exhaust gas of high H_2 content is sufficient to exaggerate ppm values even without a physical increase in pollutant production. Therefore, it is recommended to quantify emissions based on emitted pollutant mass per unit of thermal energy input.

Since no hydrogen experimental data were available, similar parameters as the NG cases were used. Figure 14 presents the obtained results given in mg/MJ. NO_x emissions generated by H_2/O_2 flame are found to be slightly higher than the NG/O_2 case. It is not straightforward to explain whether NO_x emissions increase has a physical meaning due to the presence of N_2 traces in O_2 stream, or is due to a poor NO model calibration. Accurate experimental data are therefore required to calibrate first the numerical model for hydrogen oxy-flames.

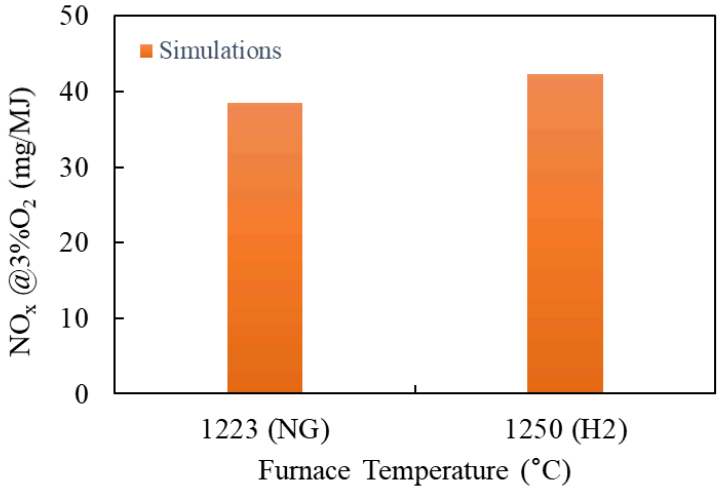

Figure 14 - Predicted NO_x emissions obtained with the reactive mixtures: NG/O_2 and H_2/O_2.

3.2.3. Synthesis

Based on the numerical results above, it can be deduced that H_2 addition results in a local increase in the flux received by the load in the first meters downstream the burner compared to the NG case. Interestingly, a series of experiments were recently conducted by Shwarz et al. [11] using an industrial high-impulse multifuel oxy-burner to investigate the effect of NG substitution with H_2. Cooling lances were introduced in the bottom of the furnace to simulate the load. The obtained results showed that the flue gas temperature decreases when switching from NG to pure hydrogen, while the heat transferred to the load increases by a few percent depending on the thermal power. A slight increase in the heat transfer to the load was also obtained by Ott et al. [12]. Caudal et al. [10] performed preliminary 1D numerical simulations of the radiative energy of combustion flue gases using an in-house internal Air Liquide tool based on the Statistical Narrow-Band (SNB) model to assess the impact on the process efficiency. A 7% increase in the power received by the load was obtained when switching from NG to H_2. All these findings are in line with the numerical results found in the present work.

Overall, replacing NG with H_2 can indeed be an effective way to reduce CO_2 emissions. Nonetheless, an in-depth analysis is required to evaluate the effect of hydrogen oxy-combustion on the product quality and how the furnace insulation behaves due to the presence of the high water vapor by-product.

4. Concluding remarks

Hydrogen could be amongst the most promising fuels to decarbonize the industry despite the technical challenges which need to be thoroughly addressed. The impact of natural gas substitution with hydrogen on heat transfer to the load and NO_x emissions are the two aspects investigated in the

present work. A numerical tool has been adapted to perform RANS simulations of the ALGLASS FC 1000 burner in the Air Liquide pilot furnace.

First, a validation of the numerical model against NG experimental data is conducted. A satisfactory agreement is obtained between experimental and numerical data at various burner thermal inputs, in terms of temperature profiles along the furnace crown, heat transfer to the load, and temperature of the flue gases. Regarding NO_x emissions, the trends are correct. However, noticeable spread between measurements and simulations persist, mainly due to the NO_x model used. The numerical model captures the physics correctly despite the differences identified and is proven to be good enough to investigate the effect of switching from NG to H_2.

The effect of hydrogen addition to natural gas is subsequently assessed by investigating two reactive mixtures (pure hydrogen and pure NG). The main key outcomes are summarized as follows:

- H_2 addition results in a local increase (up to 10%) in the flux received by the load in the first meters downstream the burner. This could be a differentiating point for some industrial applications where more heat is needed to speed up the process targeted.
- The temperature distribution in the furnace is close to that obtained with oxy-NG combustion. This means that energy distribution in the furnace is quite similar.
- Due to the relatively high temperatures generated by the oxy-H_2 flame, the presence of N_2 traces in the oxygen stream negatively impacts thermal NO_x production. It is therefore crucial to use a more accurate NO model to judge if the presence of a very limited amount of N_2 is critical when pure H_2 is used instead of NG and to improve the burner design to overcome this issue.

This study can be pushed one step further to investigate:

- The effect of burners' geometrical parameters on oxy-H_2 flame dynamics within a limited numerical cost for each tested configuration.
- Additional NG/H_2 blend ratios are needed to better apprehend the behavior of H_2 addition on the heat transfer to the load and NO_x emissions since the conversion to H_2 could be gradual in industrial furnaces (because of H_2 availability on sites). Experimental data will be necessary to further validate the numerical tool.
- Industrial furnaces are not airtight and therefore a relatively large amount of air ingress can cause additional N_2 source, which will result in NO_x formation. It would be interesting to assess the criticality of air ingress on NO_x emissions when pure H_2 is used.

5. References

[1] Kobayashi, Hisashi, Advances in oxy-fuel fired glass melting technology, In Proceedings of XX International Congress on Glass, Sep. 2004.

[2] F.R. Coelho and F.H.R França, WSGG correlations based on HITEMP2010 for gas mixtures of H_2O and CO_2 in high total pressure conditions, Int. J. Heat Mass Transfer 127 (2018) 105-114.

[3] R. Johansson, B. Leckner, K. Andersson, and F. Johnsson. Account for variations in the H_2O to CO_2 molar ratio when modelling gaseous radiative heat transfer with the weighted-sum-of-grey-gases model. Combust. Flame 158, no. 5 (2011) 893-901.

[4] F. Ammouri, C. Champinot, W. Béchara, E. Djavdan, Marc Till, and Bruno Marié, Influence of oxy-firing on the radiation transfer to the glass melting in an industrial furnace: importance of spectral radiation model, In Modélisation du rayonnement et simulation numérique des fours (Paris, 15 mai 2002), pp. D1-D16. 2002.

[5] J. A. Miller and C. T. Bowman, Mechanism and modeling of nitrogen chemistry in combustion, Prog. Energy Combust. Sci. 15, no. 4 (1989) 287–338.

[6] P. Glarborg, J. A. Miller, B. Ruscic, and S. L. Klippenstein, Modeling Nitrogen Chemistry in Combustion, Prog. Energy Combust. Sci. 67 (2018) 31–68.

[7] J. M. Samaniego, F. N. Egolfopoulos, and C. T. Bowman, Effect of chemistry and turbulence on NO formation in oxygen-natural gas flames, Cent. Turbul. Res. (1996) 187–206.

[8] Z. Li, M. Ferrarotti, A. Cuoci, and A. Parente, Finite-rate chemistry modelling of non-conventional combustion regimes using a Partially-Stirred Reactor closure: Combustion model formulation and implementation details, Appl. Energy 225 (2018) 637–655.

[9] B. Labégorre, O. Marin, O. Charon, J.M. Samaniego, T. Oguro, NOx Formation modelling in oxygen-natural gas industrial flames, American/Japanese Flame Research Committees (1998) International Symposium.

[10] J. Caudal, L. Jarry, X, Paubel, How does hydrogen fit into a carbon-free glass industry? Glass International (2024) 24-25.

[11] S. Schwarz, G. Daurer, C. Gaber, M. Demuth, R. Prieler, C. Hochenauer, Experimental investigation of the combustion characteristics in oxy-fuel combustion of hydrogen-enriched natural gas on a semi-industrial scale, Int. J. Hydrogen Energy 49 (2023) 323-337.

[12] F. Ott, J. Losacker, N. Schmitz, and H. Pfeifer. Numerical investigation of radiative transfer during oxyfuel combustion of hydrogen and hydrogen enriched natural gas in the container glass industry. In Journal of Physics: Conference Series, vol. 2685, no. 1, p. 012032. IOP Publishing, 2024.